A vision-based system for inspecting painted slates

Ovidiu Ghita, Tim Carew and Paul F. Whelan

Vision Systems Group, School of Electronic Engineering,

Dublin City University, Dublin 9, Ireland.

email: {ghitao, carewt, whelanp}@eeng.dcu.ie

Abstract

This paper describes the development of an automated vision system used to detect visual defects on painted slates. The vision system that has been developed consists of two major components covering the opto-mechanical and algorithmical aspects of the system. The first component addresses issues including the mechanical implementation and interfacing the inspection system with the sensing and optical equipment while the second component involves the development of an image processing procedure able to identify the visual defects present on the slate surface. Imaging of the slate surface poses a particular challenge because it is dark coloured, glossy, has depth profile non-uniformities, and is being transported at high speed on a conveyor. Thus, choosing an adequate illumination set–up was a key issue in the development of the vision system. The visual defects on the slate surface are detected by employing a computationally efficient four-component image–processing algorithm. The vision system is mounted on an industrial conveyor and slate inspection is carried out at production line speeds. The prototype system was subjected to robustness tests and experimental results are presented.

Keywords: Vision system, slate inspection, illumination, image processing, industrial conveyor.

1. Introduction

The aims of using automated visual inspection are to classify products for quality so that defective units may be rejected, to measure some properties of the product with a view to controlling the production process, and to gather statistics on the efficiency of the production process. Although slate manufacturing is a highly automated process, in current practice the painted slates are manually inspected by an operator who looks at them as they emerge via a conveyor from the paint process line. Hence, the aim of this work is to develop an on-line sensor capable of measuring and classifying the slates as having a surface finish of acceptable or not acceptable quality (see Whelan 1997 and Batchelor and Waltz 2001 for a review of the system engineering issues in industrial inspection).

The authors found no prior relevant work on the inspection of slates. However there is an abundance of references on the subject of inspection of ceramic tiles. Though the production processes for slates (Fernandez et al, 1998) and ceramic tiles are very different, the visual inspection process for ceramic tiles are broadly applicable to the inspection of slates as both products are rectangular in shape, have textured surfaces and arrive at the inspection point via a conveying system.

One common aspect to emerge from all the work reviewed in the field of ceramics inspection was the difficulty experienced in developing a single processing procedure to detect the wide range of defect types and sizes. The merits of a multi-component inspection were highlighted where each component is tailored to identify a specific category of defects. It is also evident from the literature review that of equal importance to the image processing procedure is the selection of an illumination set-

up that minimises spatial and temporal illumination variations. The ceramic inspection systems examined employ either diffuse or collimated lighting methods. Diffuse lighting methods were usually employed and often in combination with colour cameras. Various implementations use the diffuse lighting method to detect cracks and holes in the tile surface (Peñaranda et al 1997, Boukouvalas et al 1997). On the other hand, Boukouvalas (Boukouvalas et al 1999) employed a collimated lighting method where fluorescent lamps were used as a light source to image substrate defects such as lumps and depressions. Their imaging system relies on specular reflections where the camera and light source angles relative to normal vector of the surface being inspected are equal.

The second major component of the inspection system is the image processing algorithm that is applied to detect the visual defects. In this regard, Boukouvalas et al (1997) used 1-D convolvers to detect the spot and line defect existence on the tile surface. The optimal filter coefficients used in the convolvers can detect features with widths within a factor of 1.5 of the feature for which the filter is optimised. This is a drawback with respect to slates due to the large range of defect sizes.   More complicated techniques based on Wigner distributions are employed to inspect coloured and heavily textured tile surfaces (Boukouvalas et al, 1999). Their implementation uses a co-joint spatial frequency representation of the Wigner distribution that is used to maximise the signature of regular patterns. This method is more applicable to inspection of multi-coloured and textured surfaces and this is a limiting factor in the usefulness of this technique to slate inspection. Peñaranda (Peñaranda et al 1997) and Boukouvalas (Boukouvalas et al 1999) used grey level intensity histograms to identify whether the unit being inspected is defective. Although these methods proved to be reliable when applied to tile inspection, they are

less effective in the inspection of slates as the greyscale mean and the standard deviation vary too widely from slate to slate and within each slate.

Other related implementations include the application of the grey level difference method (Tobias et al 1995), morphological methods (Müller and Nickolay 1994), local binary pattern methods (Ojala et al 1996), (Mäenpää et al, 2003) and texture analysis (Mandriota et al, 2004), (Lu and Tsai 2005). The difference methods were ineffective because of the significant variations in acceptable grey level mean values between successive slate images. Key to the successful application of morphological methods is the selection of structuring elements matched to the size and shape of the defect features (Patek et al 1998, Whelan and Molloy 2000) and this was considered unfeasible given the vast range of defect shapes and sizes. Effective discriminatory features were not found using local binary pattern methods.

This paper is organised as follows. Section 2 describes the typical slate defects. Section 3 details the development of the prototype inspection system. Section 4 presents the adopted illumination arrangement. Sections 5 and 6 describe the image–processing algorithm. Section 7 presents several challenges introduced to the system by factory environment. Section 8 discusses the experimental results and Section 9 concludes this paper.

2. Description of slate defects

The manufactured slates are painted on a high-speed paint line and are manually inspected as they emerge from the paint line via a conveyor system. Visual inspection

is carried out manually where human inspectors make a decision as to whether each individual slate is defect free and remove the slates not meeting the inspection criteria.

The slates have a rectangular shape and their top surface is painted black or grey and has high gloss finish. The painted surface is nominally flat. The slate surface defects are broadly classified into two categories: substrate and paint. Substrate defects include incomplete slate, lumps, depressions and template marks. Paint faults include no paint, insufficient paint, paint droplets, efflorescence, paint debris and orange peel.

| (a) reference | (b) droplet | (c) spots | (d) debris | (e) template | (f) lump |
| (g) no paint | (h) effloresence | (i) shade | (j) insufficient paint | (k) template mark | (l) template mark |
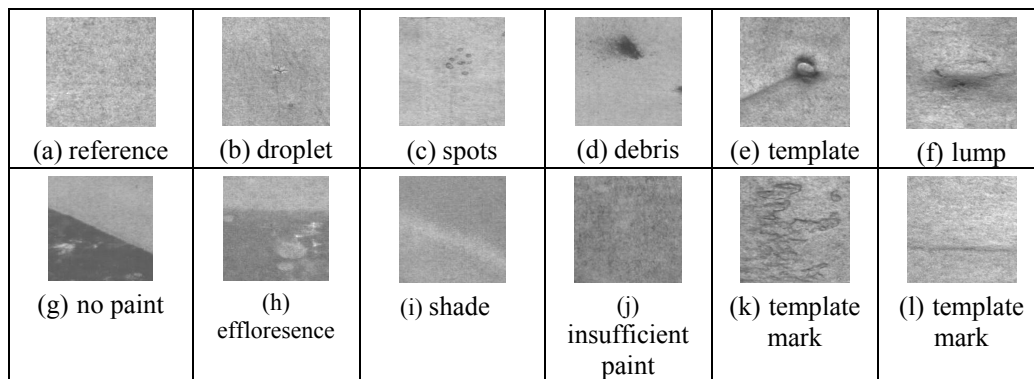
Figure 1. Representative defects found on the slate surface.

These defects can have arbitrary shapes and their sizes range from sub-millimetre to hundreds of square millimetres. A selection of representative defects is illustrated in Figure 1, where Figure 1(a) shows a defect free image section.

3. Description of the prototype inspection system

The prototype inspection system is shown in Figure 2 and was built to replicate the factory environment (for a detailed discussion the reader can refer to Newman and Jain 1995). The two meter long belt conveyor transports the slates to the inspection line at speeds in the range 15 to 50 meters per minute. The slate is illuminated using a

762 mm wide fibre optic line light where the light is collimated by a cylindrical lens. The sensing device is a Basler 2k-pixel line-scan camera fitted with a 28 mm lens. The line-scan camera operates at a scan frequency of 2.5 kHz. A micro-positioner was attached to the camera to facilitate fine adjustment of camera view line. A Euresys frame grabber is used to interface the camera to the PC. The slate is aligned by a guide placed on one side of the conveyor and an optical proximity sensor triggers the image capture immediately prior to the arrival of the slate at the inspection line. When the image transfer is complete, the slate image is processed using the image-processing routines described in Sections 5 and 6.
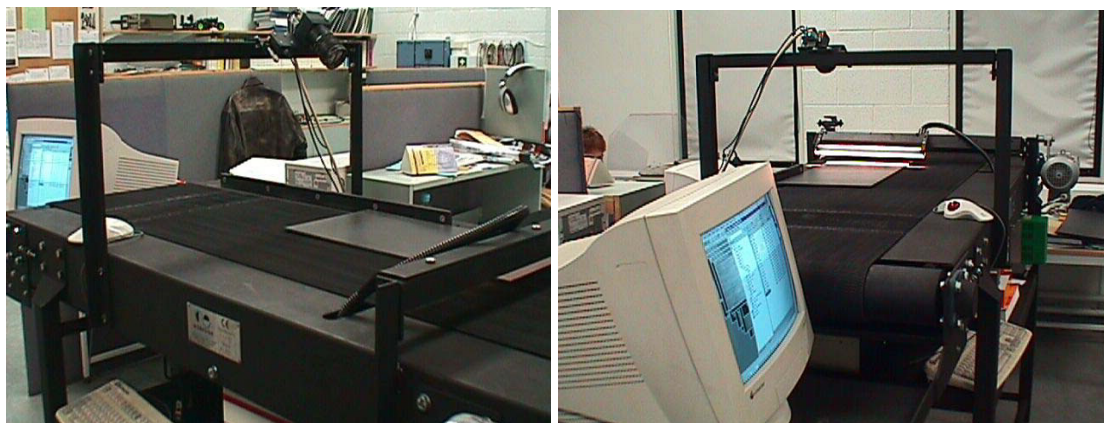
Figure 2. Conveyor and slate inspection system.

4. Illumination set-up

The strategy used to image the slate surface relies on the strong reflecting properties of the surface. Light incident on the slate will be reflected and the angle of reflection is equal to the angle of incidence if the slate surface is acceptable. The principle of operation is illustrated in Figure 3 using the Phong illumination model described by Davies (Davies 1997).
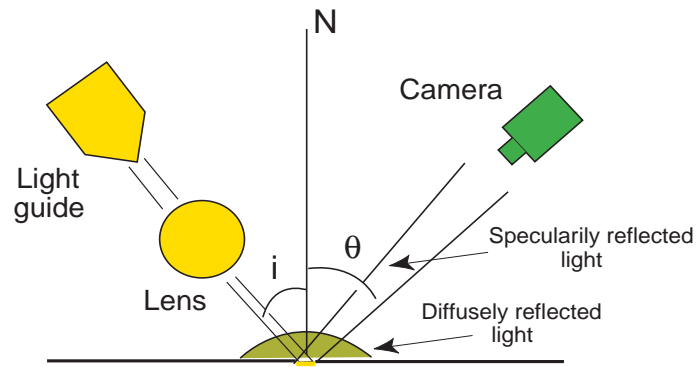
Figure 3. Model of reflectance for slate surface.

Generally speaking, paint and substrate defects have reduced gloss levels (except paint droplets that may have a higher gloss level than the slate areas of acceptable quality) or altered surface angles, and this translates to a reduction of light arriving at the sensing device. For this implementation a collimated light source was used. One of the challenging problems we encountered was the variation in depth profile across the slate due to slight but acceptable slate bowing that is sometimes present in the inspected slate. This raises and lowers the absolute position of the band of light relative to the camera view position. As a mechanical solution to force the slate into a uniform flat position is not feasible, we decided to defocus the lens used to collimate the light. This produces a wider band of light and reduces collimation. The resulting reduction in light intensity was compensated for using the spare capacity in the lamp controller. A simple trigonometric calculation was used to determine the width of the band of light required to make the system sufficiently insensitive to depth profile non-uniformities. To this end, the lens was defocused such that the resulting width of the light band was made equal to 25 mm. For this implementation the illumination set-up comprises two Fostec DCR III 150W lamp controllers, a Fostec 30" fiber optic light line and a cylindrical lens. It is useful to mention that the developed inspection system uses collimated light, and this implies that changes in the ambient light have a

negligible influence on the light reflected by the slate back to the camera. In our experiments the system was tested under various ambient lighting conditions and it was found to be insensitive to changes in the ambient lighting.

5. Segmentation of slate image from background

The first step of the devised image processing procedure involves the identification of slate boundaries. Slate edge detection was facilitated by cutting slots in the conveyor base and ensuring the belt width is less than that of the slate. The camera signal from these slots is close to the camera black level when no slate is present and there is a sharp signal transition when a slate arrives in the field of view. Therefore a simple threshold operation is sufficient to identify the slate edges. Corners are located by tracking the horizontal and vertical edge lines to their end positions.

To verify if the slate is defect free, initially, a straight line between the detected corner positions was drawn and the inspection start locations were set relative to this line. Rotation is accounted for using the equation of a straight line. After this operation the slate is segmented from the background and the four-component algorithm described in Section 6 can be applied.

6. Image processing algorithm

In order to devise an efficient solution to detect defective slates, the grey level signals from hand selected reference slates and defective slates were analysed. Experimental data indicated that the mean grey level of successive reference slates can vary by up to 20 grey levels where the average grey level was 167. These variations are not generated by imperfections in the optical or sensing equipment but rather due to acceptable variation in slate surface color. As such the image processing algorithm

has to accommodate these variations. In the next step the grey level histograms of slate images containing paint and substrate defects were investigated. This enabled us to draw a number of conclusions:

1.   The grey level mean is different for each reference slate.

2.   The limit of this variation can be determined by experimentation.

3.   The average grey level value of the defect pixels is generally lower than the average grey level value of the background pixels.

Also, it has been observed that the majority of defects are negligibly small relative to the whole slate image. This indicated that it would be desirable to inspect the slate image for defects in small image sub-sections as the relative impact of a defect on the grey level statistics of the image is increased (Fioravanti et al 1995). The slate image was divided into smaller segments of size 128 x 128 pixels and each segment was processed separately.
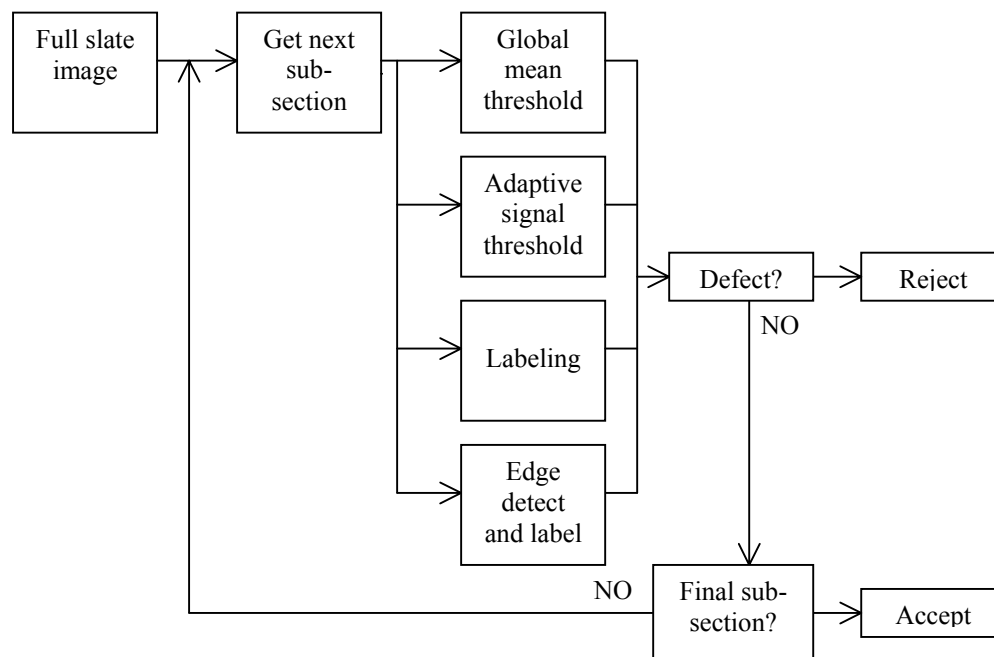
Figure 4. Slate defect detection block diagram.

The devised algorithm is illustrated in Figure 4 and consists of four distinct components with each component designed to detect specific defect types. The components are global mean threshold method, adaptive signal threshold method, labelling method and edge detection method (see Whelan and Molloy 2000 and Sonka et al 1999 for a more detailed explanation of these approaches). Each component of the algorithm is applied to each image segment and the results are compared to experimentally determined thresholds. If any result exceeds the predefined threshold then the image segment and hence the slate is considered defective. Each component of the algorithm is explained in the following sections.

6.1 Global mean threshold method

This method investigates the grey level mean of an image section. If the computed mean is lower than the experimentally determined mean then the image section belongs to a defective slate. This method is used to detect gross defects such as missing paint and orange peel. A grade-specific threshold is required for low contrast faults such as efflorescence, insufficient paint and shade variation. This method proved to be the best solution to reliably identify these types of defects.

6.2 Adaptive signal threshold method

Experimental measurements indicated that the slate texture noise is found in the band (mean − 30, mean + 30) grey levels. Also some outliers can be found in the wider band (mean − 40, mean +55) in tests on reference slates. Following extensive testing, the signal thresholds were selected as (mean - 40, mean + 60). This method was designed to detect defects such as missing paint (when less than 50% of the image section is defective), debris, droplets and spots. This method detects most substrate

defects (exceptions are shallow and thin marks). Depending on severity, defects such as efflorescence, shade variation and insufficient paint are sometimes detected.

6.3 Labelling method

Connected component labelling (Dillencourt et al 1992) is a method for detecting low contrast defects immersed in noise. This method consists of several steps (see Figure 5).
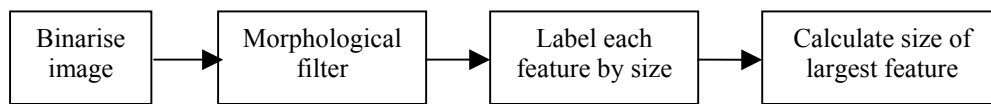
```
┌──────────┐    ┌──────────────┐    ┌──────────────┐    ┌──────────────────┐
│ Binarise │ →  │ Morphological│ →  │  Label each  │ →  │ Calculate size of│
│  image   │    │    filter    │    │ feature by size│  │ largest feature  │
└──────────┘    └──────────────┘    └──────────────┘    └──────────────────┘
```

Figure 5. Labelling method.

The first step converts the input image into binary by using a predefined threshold. By experimentation it has been found that the threshold set (mean − 15) is the most effective. The second step is applied to reduce the noise by applying a morphological opening operation. The aim of this operation is to remove the small un-connected features. The filtered image is labelled and for each connected group of pixels the algorithm assigns a unique label. The labels are ordered in accordance with the size of features. Generally speaking, the small features may be associated with slate texture and the large features may be associated with defects. In this regard, the total area of the largest ten blobs are used as the discriminative feature to classify the image section as acceptable or defective. The blob size threshold was experimentally determined. This method was effective for detection of high contrast defects such as debris, droplets, spots and no paint.

6.4 Edge detection method

The previous methods are not effective in detecting small narrow defects. Hence a fourth image processing component was added to the algorithm. Initially the image is filtered with a median filter and this is followed by the application of the Sobel edge detector. Then the image result is converted to binary by using a threshold that has been experimentally determined. The next step performs noise reduction that is achieved by applying a morphological closing operation. For this operation a 3×3 square structuring element was used to connect together the edge pixels that are situated in the 3×3 neighbourhood. The filtered image is labelled and the total area of the largest ten blobs is used to grade the image section as acceptable or defective. The sequence of operations required by this method is outlined in Figure 6.

Median filter and Sobel edge detection	Binarise and morphological filter	Label each feature by size	Calculate size of largest feature
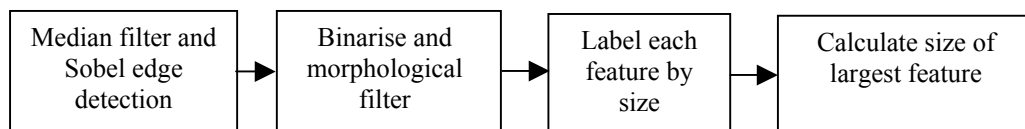
Figure 6. Edge detection method.

7. Challenges introduced by factory conditions

7.1 Effect of depth profile variation and vibration on edge detection

The devised edge detection method described in Section 5 worked very well for flat slates but resulted in false triggers for slates having significant depth profile variation. As a direct consequence, the captured image follows the curve of the slate and false rejections occur when there are large differences between the assumed straight edge and the imaged curved edge (see Figure 7). An example of false defects caused by the edge checking method is shown in Figure 8.
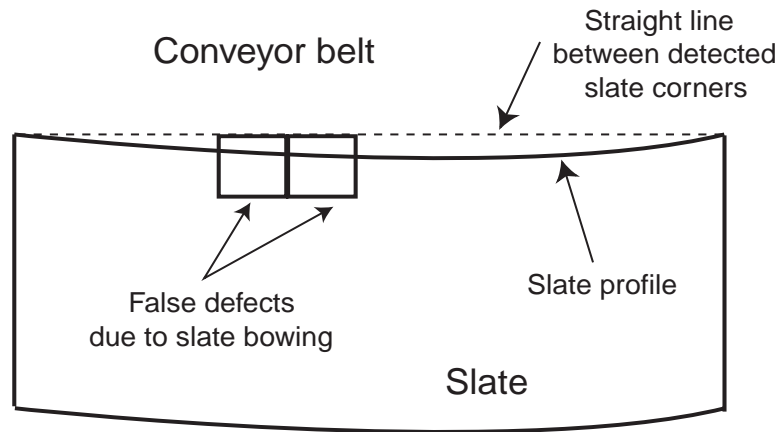
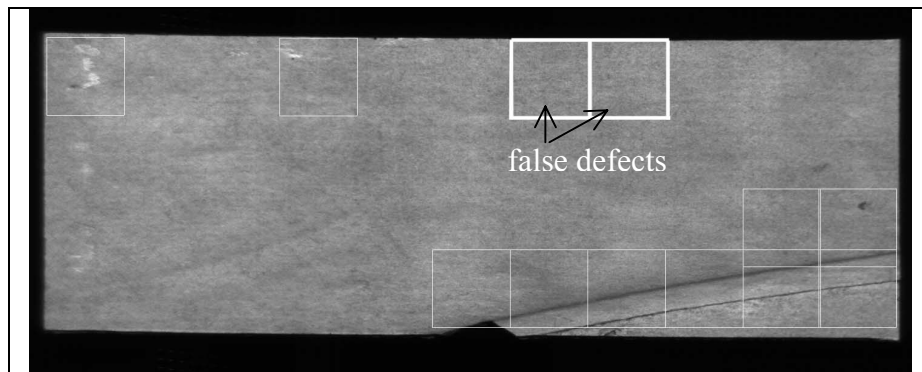Figure 7. False triggers generated by slate's depth profile variation.

Figure 8. False defect generation due to depth profile variation. The white box is drawn around 128 * 128 pixel image sub-sections considered to be defective. True positive defects are correctly detected as indicated by the faint boxes.

In order to address this problem, the slate's edge has been divided into shorter line lengths of 30 mm length and the location for these short edge segments is verified. The segmentation of slate image from the background was achieved by applying a simple threshold as explained in Section 5.

7.2 Effect of variation in speed profile

The conveyor speed was set at 38 m/min and camera exposure was set to 400 µsec giving a scan frequency of 2.5 kHz. The cross direction resolution was 0.221mm and

the moving direction resolution was 0.244 mm. The constancy of conveyor speed was measured by imaging the same slate several times and by imaging 16 slates in succession. The timing of image capture is under digital control and is repeatable. Measurements for the repeatedly imaged slate ranged from 298.3 to 300.7 mm while the measurements for 16 reference slates ranged from 295.9 to 300.1 mm. These variations are generated by the conveyor speed variations and preclude the use of image data for accurate slate measurement in the direction of travel.

8 Robustness tests

The inspection system was developed on 400 slates to determine the threshold settings that give the best trade-off between no false positive triggers and correct defect identification. Then the system was tested on more than 300 fresh slates and the success rate for correct identification of acceptable and defective slates was 99.3% for defect free slates based on 148 samples and was 97.5% for defective slates based on 162 samples.

Type	Fail qty	Pass qty	Correct result
Missing paint	0	4	100%
Insufficient paint	0	9	100%
Efflorescence	0	15	100%
Shade variation	0	12	100%
Nozzle drip	0	14	100%
Droplets	0	8	100%
Dust	0	4	100%
Wax	1	7	87%
Template marks	2	33	94%
Template marks II	0	5	100%
Lumps	0	13	100%
Depressions	1	3	75%
Bad edge	0	18	100%
Misc. types	1	12	92%
TOTAL	**5**	**157**	**97%**

Table 1. Summary of defect detection rates.

The classification of defective and defect free slates was performed by an experienced operator based on a visual examination. A detailed performance characterisation is depicted in Table 1 where the detection rate for each category of defect is presented. The efficiency of the system with respect to accepting good slates is 100%. The inspection system classified the slates containing various types of defects as defective with an overall accuracy of 97%. The system failed to identify one defective slate that had a shallow depression that was positioned parallel to the direction of slate travel. However the system was able to identify this defect when the slate was rotated with 90 degree (i.e. when the slate was imaged with the 300 mm edge facing forward) as the defect was clearly imaged. Also the system was not able to identify two slates that present tiny lumps (approx. $1mm^2$) on their surface. These defects were missed because the resolution provided by the present imaging system was not sufficient to image them accurately.
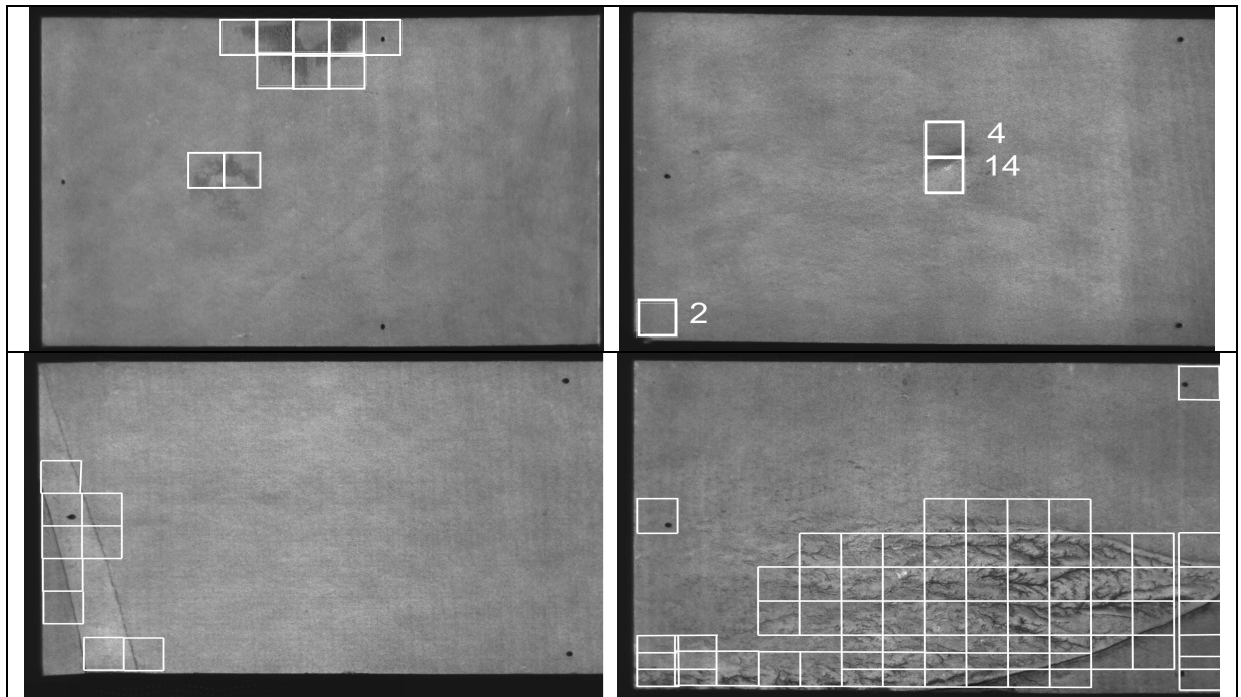
Figure 9. Typical inspection results. From top left, efflorescence, lump and damaged corner, template mark and template mark.
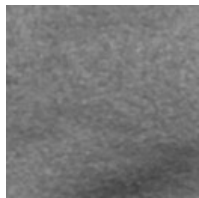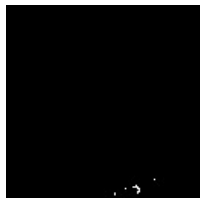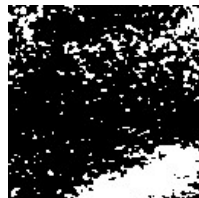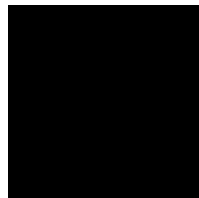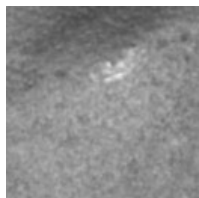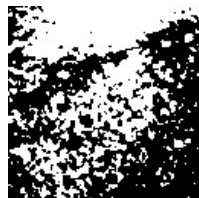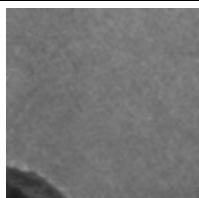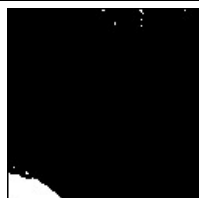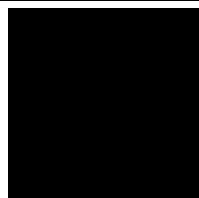
Input image	Adaptive signal component output	Threshold at (mean - 15)	Label component output	Edge component output
Threshold	38	Step 1 of label based method	900	80
Code = 4	15 OK		1738 Defect	2 OK
Code = 14	487 Defect		4020 Defect	113 Defect
Code = 2	436 Defect		538 OK	2 OK

Table 2. Image output of each algorithm component for defective image sub-sections of lump and edge fault slate shown in Figure 8.

Typical inspection results are shown in Figure 9 for defect types efflorescence, lump, damaged edge and template marks. White lines are drawn around the edges of image sub-sections found to be defective. Codes highlighting which of the algorithm components were triggered are shown for edge and lump defects in Table 2. The code for mean threshold is one, adaptive signal threshold is two, label method is four and edge method is eight. A defect can trigger more than one component. The lump defect generated a code of 14 indicating it had triggered the adaptive signal method (two), the label method (four), and the edge method (eight). The image output and

defect pixel count for the lump and edge defects of each image processing component are shown in Table 2.

Real-time operation is a realistic target although some challenges remain to produce an industrial system. The reduction of the processing time is in progress and currently the inspection takes 0.8 seconds for analysing a slate image (the algorithm was executed on a Pentium II 600 MHz PC with 128MB RAM). Also, some processing can be implemented in hardware and this will assure real-time operation.

9. Conclusions

The experimental data indicates that automating the inspection of painted slates can be achieved and installation in a factory is a realistic target. Testing the devised inspection system in a factory-type environment was an important part of the development process. It enabled us to verify that the devised mechanical system and the image-processing algorithm are feasible to be implemented in an industrial environment. The overall performance of the slate inspection system indicates that the proposed solution can be considered as a replacement for the existing manual inspection system.

Acknowledgements

References

Boukouvalas C., De Natale F., De Toni G., Kittler J., Marik R., Mirmehdi M., Petrou M., Le Roy P., Salgari R. and Vernazza F. (1997) An integrated system for quality inspection of tiles. Proc International Conference on Quality Control by Artificial Vision OCAV '97: 49-54, Toulouse, France.

Boukouvalas C., Kittler J., Marik R. and Petrou M. (1999) Colour grading of randomly textured ceramic tiles using colour histograms. IEEE Transactions on Industrial Electronics, 46(1): 219-226.

Batchelor B.G. and Waltz F.M. (2001) Intelligent Machine Vision: Techniques, Implementations and Applications. Springer Verlag, ISBN: 3540762248.

Davies E.R. (1997) Machine Vision: Theory, Algorithms, Practicalities. 2nd edition Academic Press, ISBN: 0-12-206092-X.

Dillencourt M.B., Samet H. and Tamminen M. (1992) A general approach to connected-component labeling for arbitrary image representations. Journal of the ACM, 39(2):253-280.

Fernandez C., Fernandez J. and Aracil R. (1998) Integral on-line machine vision inspection in the manufacturing process of ceramic tiles. Proc. of SPIE, Vol. 3306.

Fioravanti S., Fioravanti R., De Natale F., Marik R., Mirmehdi M., Kittler J. and Petrou M. (1995) Spectral and rank order approaches to texture analysis, European Transactions on Communications, 6(3):287-300.

Mäenpää T, Viertola J. and Pietikäinen M. (2003) Optimising colour and texture features for real-time visual inspection, Pattern Analysis and Applications, 6(3):169-175.

Mandriota C., Nitti M., Ancona N., Stella E. and Distante A. (2004) Filter-based feature selection for rail defect detection, Machine Vision and Applications, 15(4):179-185.

Lu C. and Tsai D. (2005) Automatic defect inspection for LCDs using singular value decomposition, International Journal of Advanced Manufacturing Technology, 25(1):53-61.

Müller S. and Nickolay B. (1994) Morphological image processing for the recognition of surface defects. Proc. of SPIE 2249, (58):298-307.

Newman T. and Jain A. (1995) A survey of automated visual inspection, Computer Vision and Image Understanding, 61(2):231-262.

Patek D., Goddard J.S., Karnowski T.P., Lamond D. and Hawkins T.A. (1998) Rule-based inspection of printed green ceramic tape. International Society for Optical

Engineering, Photonics West Symposium on Electronic Imaging, San Jose: 22-30.

Peñaranda J., Briones L. and Florez J. (1997) Colour machine vision system for process control in ceramics industry. Proc. of SPIE 3101: 182-192.

Ojala T., Pietikäinen M. and Harwood D. (1996) A comparative study of texture measures based on feature distributions. Pattern Recognition, 29(1): 51-59.

Sonka M., Hlavac V. and Boyle R. (1999) Image Processing, Analysis, and Machine Vision. 2nd edition, PWS Publishing, ISBN: 0-534-95393-X.

Tobias O., Seara R., Soares F. and Bermudez J. (1995) Automated visual inspection using the co-occurrence approach. IEEE Midwest Symposium on Circuits and Systems:154-157.

Whelan P.F. (1997) System engineering issues in industrial inspection. IEE Colloquium on Industrial Inspection, (Digest) (41):1-5.

Whelan P.F. and Molloy D. (2000) Machine Vision Algorithms in Java, Techniques and Implementation. Springer (London), ISBN: 1-85233-218-2.

Ovidiu Ghita received his B.E. and M.E. degrees in Electrical Engineering from Transilvania University, Brasov, Romania. From 1994 through 1996 he was an Assistant Lecturer in the Department of Electrical Engineering at Transilvania University. Since then, he has been a member of the Vision Systems Group at Dublin City University (DCU), during which time he received his Ph.D. for work in the area of robotic vision. Currently, he holds a position of postdoctoral Research Assistant in the Vision Systems Group at DCU. His current research interests are in the area of range acquisition, machine vision and medical imaging.

Tim Carew received his B.Eng. from Dublin City University in 1985. Since then he was employed in Tokyo by the Japanese company KGK until 1992, principally working on laser and CCD camera based inspection systems. From 1993 until 2000, he developed web inspection solutions at TSI Ltd, Dublin, Ireland and completed his M.Eng at Dublin City University in 2002. Currently he explores his research interests through TSI.

Paul F Whelan received his B.Eng.(Hons) degree from the National Institute for Higher Education Dublin, a M.Eng. degree from the University of Limerick, and his Ph.D. (Computer Science) from the University of Wales, Cardiff. During the period 1985-1990 he was employed by Industrial and Scientific Imaging Ltd and later Westinghouse (WESL), where he was involved in the research and development of industrial vision systems. He was appointed to the School of Electronic Engineering, Dublin City University (DCU) in 1990 and currently holds the position of Associate Professor. As well as a wide range of scientific publications, Prof. Whelan co-edited *Selected Papers on Industrial Machine Vision Systems* (1994), and was the co-author

of *Intelligent Vision Systems for Industry* (1997) and *Machine Vision Algorithms in Java* (2000). His research interests include applied morphology, texture analysis, machine vision and medical imaging. He is a Senior Member of the IEEE, a Chartered Engineer and a member of the IEE and IAPR. He served on the IEE Irish centre committee (1999-2002) and is member of the governing board of the *International Association for Pattern Recognition (IAPR)* and as the President of the *Irish Pattern Recognition and Classification Society.*